

Multisensor Observation and Simulation of Snowfall During the 2003 Wakasa Bay Field Experiment

Benjamin T. Johnson* (jbenjam@aos.wisc.edu)¹, Grant W. Petty¹,
Gail Skofronick-Jackson², and James W. Wang²

¹ Atmospheric and Oceanic Sciences Department, University of
Wisconsin, Madison, WI 53706

² NASA Goddard Space Flight Center, Code 975, Greenbelt, MD 20771

This research seeks to assess and improve the accuracy of microphysical assumptions used in satellite passive microwave radiative transfer models and retrieval algorithms by exploiting complementary observations from satellite radiometers, such as TRMM/AMSR-E/GPM, and coincident aircraft instruments, such as the next generation precipitation radar (PR-2). We focus in particular on aircraft data obtained during the Wakasa Bay field experiment, Japan 2003, pertaining to surface snowfall events. The observations of vertical profiles of reflectivity and Doppler-derived fall speeds are used in conjunction with the radiometric measurements to identify 1-D profiles of precipitation particle types, sizes, and concentrations that are consistent with the observations.

Introduction

In the mid- to high-latitudes, the spatial structure and microphysics of precipitating clouds differ significantly from that of tropical and warm-cloud precipitation (1). The variety of precipitation particles, low precipitation rates, surface snow-cover, and low freezing level heights all contribute to additional uncertainties involving passive microwave (PMW) precipitation retrievals (2). To date, very few coincident aircraft and microwave observations have been made of mid-to-high latitude cold-cloud precipitation.

The key research questions to be briefly addressed in this paper are:

1. What are the *ranges* of microphysical features, such as particle shapes, fall speeds, composition, and sizes, of mid- to high-latitude cold-cloud precipitation?
2. What are the primary physical relationships between the microphysics and microwave radiative transfer?
3. To what degree can independent observations, for example, aircraft Doppler radar, be used to improve the accuracy of PMW precipitation retrievals?
4. To what extent and under what conditions can existing PMW methods reliably infer details of these precipitating systems?

We employ aircraft observations of snowfall obtained during the Wakasa Bay experiment using data from the following instruments: 2nd generation Precipitation Doppler Radar (PR-2) operating at 13.4 GHz and 35.6 GHz; Polarimetric Scanning Radiometer (PSR) at 10.7, 18.7, 37.0, and 89.0 GHz; Airborne Cloud Radar

(ACR) at 94 GHz; and the Millimeter-wave Imaging Radiometer (MIR) at 89, 150, $183.3 \pm (1, 3, 7)$, 220, and 340 GHz. Satellite observations from the Advanced Microwave Scanning Radiometer for EOS (AMSR/E) are also used when reasonable spatial and temporal co-location is possible.

Information inferred from the aircraft observations are used to constrain assumptions and parameterizations in a *forward model* (i.e., simulation of microwave radiances), which in turn imposes constraints on the set of solutions computed by a precipitation retrieval algorithm (i.e., the inverse of forward model).

Simulation / Forward Model

The forward model provides a basis for simulating passive microwave brightness temperatures (TBs) and radar reflectivities for a 1-D vertical precipitation profile. The three primary components of the forward model are the: *physical model*, *hydrometeor model*, and *radiative transfer model* (RTM).

1-D Physical Model: The parametric, one dimensional physical model described in (3) is employed with modifications. A number of reasonable constraints are applied to limit the number of free parameters describing the 1-D column of precipitation. Figure (1a) illustrates an example of precipitation rate as a function of height for pristine snowflakes and aggregates (70% ice by volume). Figure (1b) shows the 3 GHz simulated radar reflectivity and the Sekhon Srivastava Z-R relationship for comparison.

Hydrometeor Model: Precipitation hydrometeors are most commonly modeled as homogeneous dielectric spheres, so that standard Mie codes may be utilized to compute local radiative transfer properties, such as single scattering albedo (ϖ_0), asymmetry parameter ($\langle g \rangle$), and mass extinction coefficient ($\langle k_{\text{ext}} \rangle$). See, for example, (3). Each particle is simulated as an effectively homogeneous dielectric sphere of mass M composed of a blend of liquid, ice, and air; with volume fractions F such that $F_{\text{liq}} + F_{\text{ice}} + F_{\text{air}} = 1$. The density is an average of the individual components (neglecting the mass of air) where $\rho \approx F_{\text{liq}} \rho_{\text{liq}} + F_{\text{ice}} \rho_{\text{ice}}$. The melted-equivalent particle diameter is $D = (3M/(4\rho_{\text{liq}}))^{1/3}$. The physical diameter is $D' = D (\rho_{\text{liq}}/\rho)^{1/3}$. Averaging of the dielectric function uses the effective medium approximation, and generalized to three components.

The distribution of particle sizes is the exponential distribution, given by $N(D) = N_0 \exp[-\Lambda D]$. Integration over all diameters yields the total number of particles per unit volume of air. The total mass of water per unit volume of air is, therefore, $W = \frac{\pi \rho_{\text{liq}}}{6} \int_0^\infty D^3 N(D) dD$. In the absence of vertical motion, the precipitation rate is $\mathcal{R} = W \langle v \rangle / \rho_{\text{liq}}$, where $\langle v \rangle$ is the mass-weighted average of the particles' terminal fallspeed. For dry snowflakes, observed fall speeds are on the order of 1 m/s. Aggregates and graupel range up to about 3 m/s (cf., Rogers and Yau, Figure 9.7).

1-D Radiative Transfer Model: The radiative transfer model used for this research is the plane-parallel, fully polarized, adding-doubling radiative transfer model, RT4 (4).

It incorporates surface scattering/emission, and multiple independent layers. Example brightness temperature results for the 1-D model are presented in Figure (1c). TB values at common microwave channels are plotted for clear sky (open circles, water vapor attenuation only) and a precipitating cloud (Figure 1a). The brightness temperature depression at 89V and 150V (solid circle and line) indicates scattering by frozen precipitation, whereas lower frequency microwaves are relatively insensitive to scattering by frozen hydrometeors.

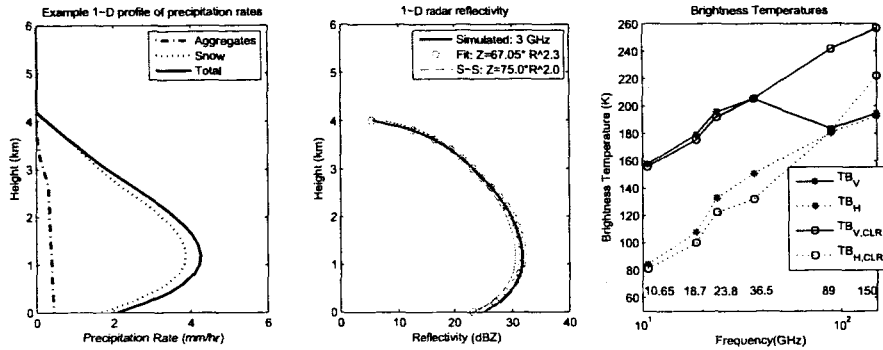


Figure 1: Simulated 1-D profile for snowfall rate, radar reflectivity, and brightness temperatures (51°, over ocean) from the forward model.

Observations

Figure 2 shows an example snow case observed by the PR-2 over ocean during the Wakasa bay field experiment. The 13.4 GHz and 35.6 GHz reflectivities, nadir Doppler velocity, and linear depolarization ratio (at 13.4 GHz) are plotted versus height. 4-5 distinct snow storms are apparent in this image: no radar brightband is visible and Doppler velocities are mostly confined to the 1-3 m/s range – consistent with expected values for snowflakes and aggregates. The 13.4 GHz channel is sensitive to larger particles but is less susceptible to attenuation through clouds and water vapor. Smaller particles scatter microwaves from the 35.6 GHz channel, however, attenuation is greater and the reflectivities are generally smaller in comparison to the 13.4 GHz channel.

Other instruments, such as the ACR, MIR, and PSR provide coincident and complementary datasets, and will be incorporated into the research as necessary and available.

Comparison Plan and Discussion

PR-2 retrievals of particle size distribution (PSD) parameters are performed using the methods of (5), and will be incorporated into a database of simulated 1-D model profiles, brightness temperatures, and simulated PR-2 radar profiles – an example of which was shown in Figure 1. However, we do not seek to identify specific PSD parameters on a case-by-case basis, but rather identify realistic range bounds on PSD parameters for “typical” mid-latitude cold-cloud precipitation cases over

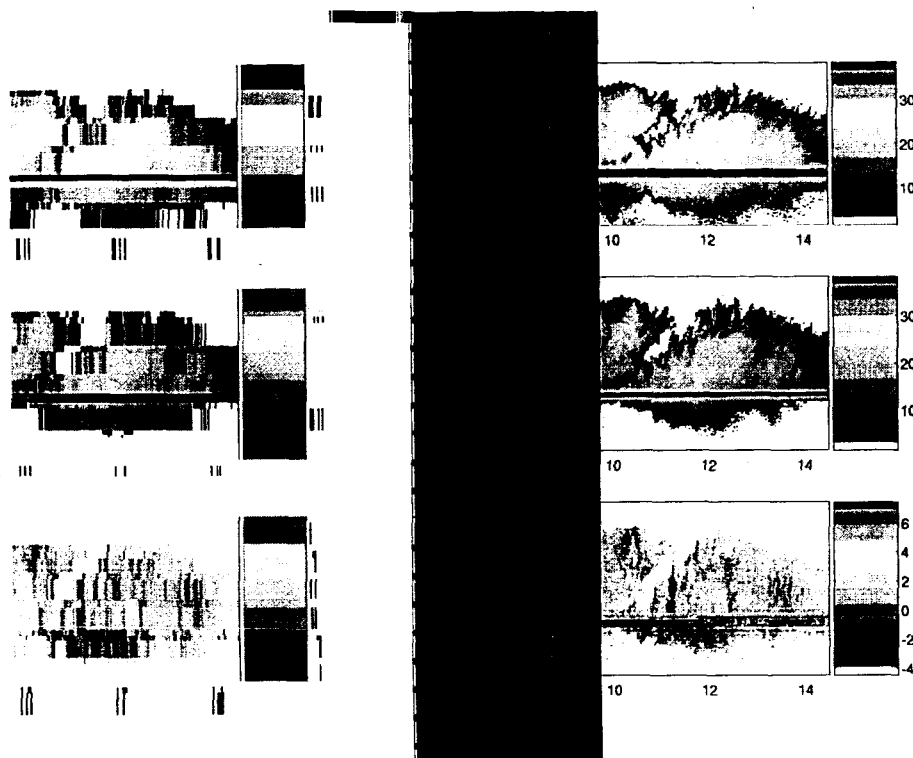


Figure 2: PR-2 Observations – 1/29/2003 starting 03:18:42 UTC

ocean and land. One can then match database TBs (and associated profiles) with satellite-based passive microwave observations to improve the accuracy of precipitation retrieval algorithms.

References

- [1] R. A. Houze, Jr, *Cloud Dynamics*, Academic Press, 1993.
- [2] T. T. Wilheit, C. D. Kummerow, and R. R. Ferraro, "Rainfall algorithms for AMSR-E," *IEEE T. Geosci. Remote*, vol. 41, no. 2, pp. 204–214, 2003.
- [3] G. W. Petty, "Physical and microwave radiative properties of precipitating clouds. Part II: A parametric 1d rain-cloud model for use in microwave radiative transfer simulations," *J. Appl. Meteorol.*, vol. 40, no. 12, pp. 2115–2129, 2001.
- [4] K. F. Evans, J. Turk, T. Wong, and G. L. Stephens, "A Bayesian Approach to Microwave Precipitation Profile Retrieval," *J. of Appl. Meteorol.*, vol. 34, no. 1, pp. 260–280, 1995.
- [5] R. Meneghini, H. Kumagai, J. R. Wang, T. Iguchi, and T. Kozu, "Microphysical retrievals over stratiform rain using measurements from an airborne dual-wavelength radar-radiometer," *IEEE Trans. Geosci. Remote Sens.*, vol. 35, no. 3, pp. 487–506, 1997.